

## Magnetic x-ray scattering measurements on $\text{MnF}_2$

A. I. Goldman, K. Mohanty, and G. Shirane

*Brookhaven National Laboratory, Upton, New York 11973*

P. M. Horn and R. L. Greene

*IBM Thomas J. Watson Research Center, Yorktown Heights, New York 10598*

C. J. Peters, T. R. Thurston, and R. J. Birgeneau

*Department of Physics, Massachusetts Institute of Technology, Cambridge, Massachusetts 02139*

(Received 25 March 1987)

We report the results of a high-resolution synchrotron x-ray scattering study of the magnetic scattering from  $\text{MnF}_2$ . The temperature dependence of the magnetic order parameter was obtained from the intensity of the direct magnetic scattering of x rays from the  $\text{Mn}^{2+}$  spins. The intense, highly collimated synchrotron beam allowed for a clear, extinction-free separation of the Bragg component from the diffuse scattering even very close to the Néel temperature  $T_N$ . The excellent magnetic scattering signal-to-noise ratio should allow for the observation of critical scattering for temperatures within 1 mK of  $T_N$ .

### INTRODUCTION

The availability of high-intensity synchrotron radiation has stimulated rapid progress in the study of magnetic structures using x rays. In particular, since the pioneering experiments of DeBergevin and Brunel,<sup>1</sup> using a conventional x-ray source, high-resolution measurements of magnetic scattering from holmium and erbium by Gibbs and co-workers<sup>2,3</sup> have led to a new model of the magnetic structure of rare-earth metals. Vettier *et al.*<sup>4</sup> have employed the tunability of the x-ray energy from a synchrotron source to maximize the interference between the charge and magnetic cross section in a measurement of the modulation of the magnetic moment in the Gd-Y superlattice structures. In this paper, we concern ourselves with measurements of the sublattice magnetization, and the feasibility of studying critical scattering from the well-known uniaxial antiferromagnet  $\text{MnF}_2$ .

Studies of the sublattice magnetization and critical scattering have traditionally fallen within the realm of neutron scattering techniques since the cross section from magnetic scattering using neutrons is of the same order as the nuclear cross section. In addition, the kinetic energy of thermal neutrons is well suited to the investigation of low-energy excitations in magnetic materials, allowing one to probe both the static and dynamic consequences of the magnetic interactions. However, the moderate angular resolution feasible in neutron studies has hindered accurate measurements of the sublattice magnetization and critical scattering as the Néel temperature is closely approached. The high resolution allowed by the high intensity and intrinsic collimation of synchrotron sources allows a cleaner separation of the Bragg component from the diffuse critical scattering over a wider range of reduced temperature and, in principle, should extend the range of observation to within 1 mK of the critical temperature. For high-quality crystals, neutron Bragg peak intensities are also strongly affected by extinction. By

contrast, the minuteness of the magnetic cross section for x rays, as compared to the absorption cross section for  $\text{MnF}_2$ , allows an *extinction-free* measurement of the sublattice magnetization to be made from the lowest obtainable temperature up to the critical temperature.

$\text{MnF}_2$  is one of the most thoroughly investigated antiferromagnetic compounds. A variety of techniques, including neutron scattering,<sup>5</sup> antiferromagnetic resonance,<sup>6</sup> specific-heat measurements,<sup>7</sup> and nuclear magnetic resonance<sup>8</sup> has been employed to study both the critical region near  $T_N$  and the lower-temperature spin-wave behavior.  $\text{MnF}_2$  has a simple tetragonal crystal structure with the  $\text{Mn}^{2+}$  ions forming a body-centered lattice.<sup>9</sup> Below  $T_N$ , the Mn spins at the body-center and corner sites align antiferromagnetically with the weak anisotropy, due to dipole interactions orienting the spins along the  $c$  axis.<sup>10</sup> The magnetic unit cell is the same as the chemical unit cell. Even though  $\text{MnF}_2$  is a simple tetragonal, the  $\text{Mn}^{2+}$  and  $\text{F}^-$  ions occupy sites such that charge scattering is forbidden when two of  $h$ ,  $k$ , and  $l$  are 0 and  $h+k+l=2n+1$ . This holds even for any charge scattering induced by the magnetic order. Thus the magnetic scattering is most conveniently studied at the (100) reflection.

### EXPERIMENTAL DETAILS

The  $\text{MnF}_2$  single crystal used in this investigation was grown by Linz of MIT, and used in previous neutron scattering studies of critical scattering by Schulhof, Heller, Nathans, and Linz.<sup>5</sup> For the present study, a face parallel to the (100) planes of the crystal was cut and polished. X-ray rocking-curve measurements of the (200) reflection from the face demonstrated the integrity of the crystal after this treatment; the mosaic was less than  $0.005^\circ$  half width at half maximum (HWHM). The sample was mounted in a Be can on the cold finger of a

closed-cycle Displex refrigerator. The temperature stability was measured to be  $\pm 5$  mK over the course of a typical scan of up to 1.5 h.

Measurements of the magnetic scattering at the (100) and (300) reciprocal-lattice points were made on beamline X-20A at the National Synchrotron Light Source at Brookhaven National Laboratory. The beam was focused on the sample with a platinum-coated Si mirror and monochromatized with two Si(111) crystals. The beam flux on the sample was about  $2 \times 10^{11}$  photons/sec $\text{mm}^2$ . A Si(111) crystal was used in the analyzer position leading to a nondispersive longitudinal resolution of about  $4 \times 10^{-4}$   $\text{\AA}^{-1}$  HWHM at  $K_i = 3.043$   $\text{\AA}^{-1}$ . The longitudinal scans of the  $\text{MnF}_2$  (200) Bragg peak were resolution limited with widths of about  $4.6 \times 10^{-4}$   $\text{\AA}^{-1}$  HWHM. The Displex was mounted on a four-axis Huber spectrometer with the  $\text{MnF}_2$  crystal oriented with the [001] axis perpendicular to the scattering plane; the polarization of the incident radiation was then along the unique magnetic axis of the sample.

There are two major technical difficulties inherent in measuring the weak magnetic signal at the antiferromagnetic Bragg positions. Although charge scattering is nominally forbidden at these points, parasitic peaks in the form of harmonic contamination and, more seriously, multiple scattering hinder useful measurements. The contribution from higher-energy harmonics in the incident beam was effectively eliminated by choosing the primary energy (6 keV) diffracted from the Si(111) monochromator such that the third- and higher-order reflections were diffracted at an energy above the 12-keV cutoff of the mirror. Elimination of multiple scattering is more difficult. However, by a suitable choice of incident energy, and by a very careful rotation of the crystal about the scattering vector, we were able to find regions which were, in fact, relatively free of multiple scattering.

## RESULTS AND ANALYSIS

Figure 1 shows longitudinal scans through the magnetic (100) reflection from  $\text{MnF}_2$  taken at two temperatures. At 50 K the peak counting rate is approximately 20 counts/sec, while the background is on the order of 0.6 counts/sec, so that the signal-to-noise ratio at this temperature is about 33:1. A comparison of the integrated intensity of the magnetic signal shown in Fig. 1 with the (200) Bragg peak shows that the magnetic scattering cross section at 50 K is on the order of  $10^{-5}$  of the charge scattering cross section. This value represents an upper limit to the ratio of the two cross sections since the intensity from the (200) peak has not been corrected for extinction effects which are probably significant. The resolution-limited width of this peak requires that the antiferromagnetic domain size exceed 10000  $\text{\AA}$ .

At the lowest temperature measured, 13 K, the count rate in the magnetic Bragg peak was approximately 40 counts/sec, yielding an excellent and somewhat unanticipated signal-to-noise ratio of about 70:1. Near the Néel temperature, we expect the critical diffuse scattering contribution to be on the order of a few percent of the low-temperature Bragg scattering, so that the signal rates ex-

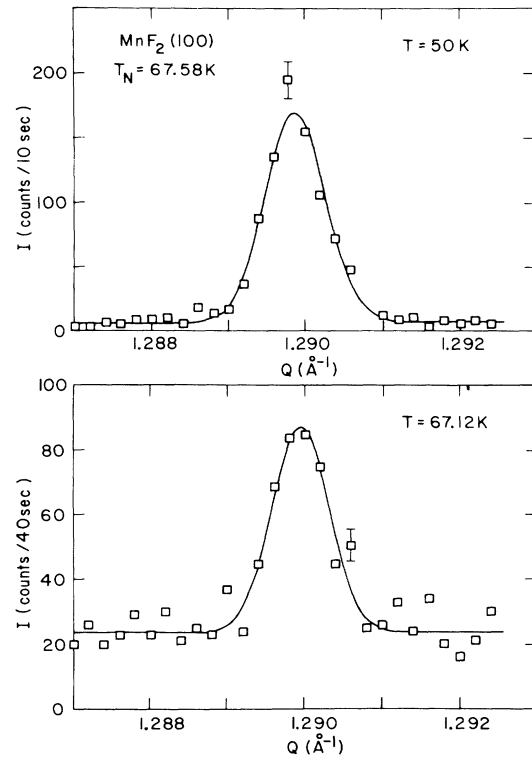


FIG. 1. Longitudinal ( $Q$ ) scan through the magnetic (100) peak at  $T=50$  and 67.12 K. The solid lines are the results of least-squares fits of Gaussian profiles to the data. Both peaks have width  $\Delta Q = 4.6 \times 10^{-4}$   $\text{\AA}^{-1}$  (HWHM). Data were obtained for constant monitor counts. A typical counting time was 10 sec per 100-K monitor for ring currents of 100 mA.

pected in the diffuse peak will be comparable, or slightly greater than the background. This rough estimate is appropriate to the case where there is a good match between the angular distribution of the diffuse scattering, and the extent of the experimental resolution. Clearly, for cases where the resolution is much sharper than  $\kappa$ , the inverse correlation length, the diffuse component will be more difficult to observe. As we discuss further below, this places significant constraints on the range of reduced temperatures at which critical scattering is significant and makes possible accurate order-parameter measurements quite close to  $T_N$ .

In Fig. 2, we plot as filled circles the temperature dependence of the peak intensity at the (300) reflection. We remind the reader that as long as the width of the Bragg component is constant, the peak intensity scales directly with the integrated intensity, which is a measure of the square of the sublattice magnetization. The upper panel shows data over the entire temperature range, while the lower panel shows data near  $T_N$ . The solid lines represent the square of the magnetic order parameter as measured by NMR.<sup>8</sup> Two parameters have been adjusted in this comparison,  $T_N$  and the absolute magnitude of the low-temperature order parameter. The agreement is obviously excellent. The Néel temperature determined here,  $67.58 \pm 0.01$  K, is within 0.12 K of that measured by

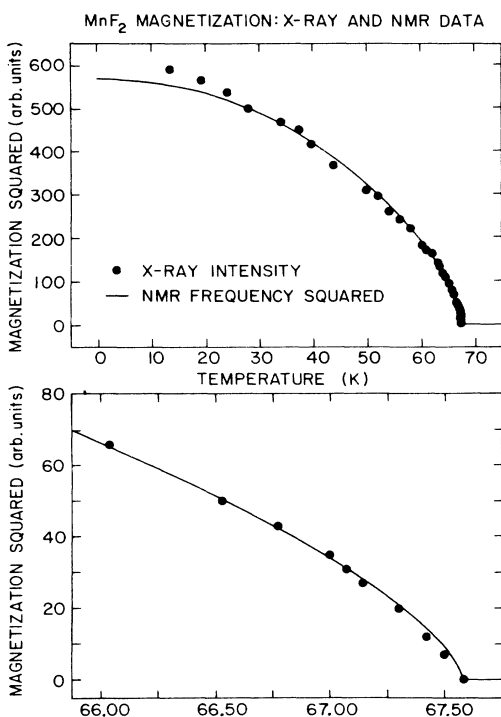


FIG. 2. Peak intensity at the magnetic (300) Bragg point (filled circles) as a function of temperature. The solid lines represent the square of the magnetic order parameter as measured by NMR (Ref. 8).

Schulhof *et al.*,<sup>5</sup> the difference may be attributed to errors in the absolute calibration of the thermometers. The best-fit critical exponent for the sublattice magnetization,  $\beta = 0.31 \pm 0.02$ , is in good agreement with measurements by other techniques and with theory for the three-dimensional Ising model.<sup>11</sup> Given this agreement and the quality of the data, it is clear that magnetic x-ray scattering provides a reliable measure of the magnetic order parameter over the entire temperature range.

Finally, we discuss some preliminary data taken in the immediate vicinity of  $T_N$ . In Fig. 3 we show a radial scan of the magnetic (100) peak for  $T \approx T_N$ . The solid line represents the best fit of a Gaussian line shape to the data with the width constrained at its low-temperature value  $4.6 \times 10^{-4} \text{ \AA}^{-1}$  HWHM. The dashed line represents a fit with arbitrary width. It is clear that the dashed line gives a better description of the data. However, the measured linewidth is far too small to be accounted for as simple magnetic critical scattering. From the neutron critical scattering results of Schulhof *et al.*<sup>5</sup> we estimate that at  $T_N - T = 0.32 \text{ K}$ , the HWHM of the diffuse scattering should be about  $0.03 \text{ \AA}^{-1}$ , significantly greater than the measured broadening. It is possible that the broadening is a result of disorder in the surface region of the crystal due to the polishing of the crystal, although it is difficult to ascertain why the effect only manifests itself very near  $T_N$ . Unfortunately, our experimental temperature control

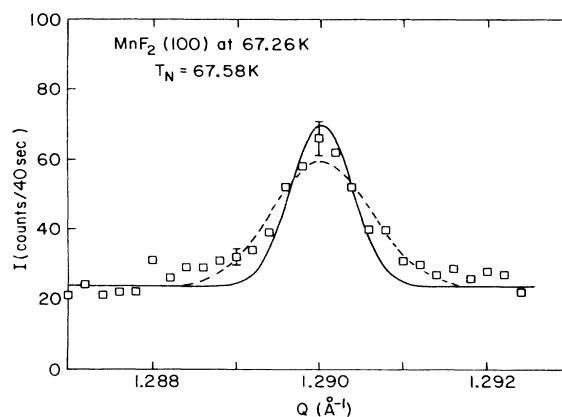


FIG. 3. Longitudinal ( $Q$ ) scan through the magnetic (100) peak for  $T = 67.26 \text{ K}$ . The solid line represents the results of a least-squares fit of a Gaussian profile to the data with the width constrained at  $\Delta Q = 4.6 \times 10^{-4} \text{ \AA}^{-1}$ . The dashed line represents a fit of a Gaussian with arbitrary width.

was not sufficient to monitor this effect accurately. Therefore, a more detailed study of this phenomenon must await a separate experiment.

In conclusion, we have demonstrated the ability of direct magnetic x-ray scattering to provide an accurate, extinction-free measurement of magnetic order parameters at high resolution. Future work could extend these measurements within 1 mK of  $T_N$ , into regions inaccessible to neutron measurements. Further, since the penetration depth of the x-ray beam is only about  $20 \mu\text{m}$ , accurate measurements on thin-film materials will also be possible. This should be especially important in random alloys where macroscopic concentration gradients often represent the limiting factor in accurate characterization of the phase transition behavior.

#### ACKNOWLEDGMENTS

We are grateful to A. Aharony, A. S. Arrott, J. D. Axe, G. B. Benedek, L. D. Gibbs, D. Mukamel, L. Passell, and C. Stassis for stimulating discussions. We greatly appreciate the efforts of J. Hurst in sample preparation, and P. W. Stephens for his contribution to the early stages of this project. Work at Brookhaven was supported by the Division of Materials Sciences, U. S. Department of Energy under Contract No. DE-AC02-76-CH00016, and at MIT by the National Science Foundation, Low Temperature Physics Program under Grant No. DMR85-01856. One of us (T.R.T) would like to acknowledge support from the National Science Foundation. The National Synchrotron Light Source is supported by the U. S. Department of Energy, Division of Materials Sciences and Division of Chemical Sciences. The MIT part of the IBM/MIT consortium is supported by the National Science Foundation, Materials Research Laboratory under Grant No. DMR84-18718.

- <sup>1</sup>F. DeBergevin and M. Brunel, Phys. Lett. **39A**, 141 (1972); Acta Crystallogr. A **37**, 314 (1980); M. Brunel and F. DeBergevin, *ibid.* A **37**, 324 (1980).
- <sup>2</sup>D. Gibbs, D. E. Moncton, K. L. D'Amico, J. Bohr, and B. H. Grier, Phys. Rev. Lett. **55**, 234 (1985).
- <sup>3</sup>D. Gibbs, J. Bohr, J. D. Axe, D. E. Moncton, and K. L. D'Amico, Phys. Rev. B **34**, 8182 (1986).
- <sup>4</sup>C. Vettier, D. B. McWhan, E. M. Gyorgy, J. Kwo, B. M. Buntschuh, and B. W. Batterman, Phys. Rev. Lett. **56**, 757 (1986).
- <sup>5</sup>M. P. Schulhof, P. Heller, R. Nathans, and A. Linz, Phys. Rev. **B 1**, 2304 (1970); **4**, 2254 (1971).
- <sup>6</sup>F. M. Johnson and A. H. Nethercot, Jr., Phys. Rev. **114**, 705 (1959).
- <sup>7</sup>D. T. Teany, Phys. Rev. Lett. **14**, 898 (1965).
- <sup>8</sup>P. Heller, Phys. Rev. **146**, 403 (1966).
- <sup>9</sup>M. Griffel and J. W. Stout, J. Am. Chem. Soc. **72**, 4351 (1950).
- <sup>10</sup>R. A. Erickson, Phys. Rev. **90**, 779 (1953).
- <sup>11</sup>M. E. Fisher and Jing-Huei Chen, J. Phys. (Paris) **46**, 1645 (1985).